7

Species–Area Relationships and Diversity Measures in the Forest Dynamics Plots

Richard Condit, Egbert G. Leigh, Jr., Suzanne Loo de Lao, and CTFS Working Group*

Species–area and species–individual curves show how species accumulate with increased sample size (Rosenzweig 1995). If the curves have a specific form, they provide a means for predicting the number of species in larger areas with data from small samples. For example, if curves follow a power function, meaning they are linear on a log-log scale, then extrapolation to large areas is straightforward. Condit et al. (1996, 1998) examined species–individual curves in three large Forest Dynamics Plots and showed that the power function does not hold in samples less than about 10,000 individuals. For the three plots, the form of the species–individual curve is much better predicted by the equation for Fisher's α:

$$S = \alpha \ln\left(1 + \frac{N}{\alpha}\right), \tag{7.1}$$

where S is the number of species in a sample of N individuals, and α is a constant, Fisher's α, which is independent of N (see part 5, Introduction). On a log-log scale, the species–individual curve ascends steeply initially, but its slope diminishes progressively thereafter.

Fisher's α is frequently used as a diversity parameter (Fisher et al. 1943; Rosenzweig 1995; Condit et al. 1998). This parameter has a curious history. Fisher et al. (1943) found that in catches of moths at light traps, the distribution of individuals over species followed the log series: The number $S(m)$ of moth species with m sampled individuals apiece is $\alpha x^m/m$, where α is Fisher's α and x depends on N. This same log series also applies in a neutral community of N trees where, at each time-step, a tree chosen at random dies, another is chosen at random to be the

*For this book, the CTFS Working Group includes: P. S. Ashton, N. Brokaw, S. Bunyavejchewin, R. Condit, G. Chuyong, L. Co, H. S. Dattaraja, S. Davies, S. Esufali, C. Ewango, R. Foster, N. Gunatilleke, S. Gunatilleke, T. Hart, C. Hernandez, S. Hubbell, A. Itoh, R. John, M. Kanzaki, D. Kenfack, S. Kiratiprayoon, J. LaFrankie, H. S. Lee, I. Liengola, S. Lao, E. Losos, J. R. Makana, N. Manokaran, H. Navarrete, T. Ohkubo, R. Pérez, N. Pongpattananurak, C. Samper, Kriangsak Sri-ngernyuang, R. Sukumar, I.-F. Sun, H. S. Suresh, S. Tan, D. Thomas, J. Thompson, M. Vallejo, G. Villa Muñoz, R. Valencia, T. Yamakura, J. Zimmerman.

seed-parent of the immediately maturing young that replaces the dead tree, and this young has probability v of being an entirely new species (Watterson 1974, Hubbell 2001).

Where the log series applies, the number of trees belonging to a species with m trees apiece is $mS(m) = \alpha x^m$, the total number of trees sampled is

$$N = \sum_{m=1}^{\infty} mS(m) = \sum_{m=1}^{\infty} \alpha x^m = \frac{\alpha x}{1-x},$$

and $x = N/(N+\alpha)$. Similarly, the number S of species in the sample is

$$S = \sum_{m=1}^{\infty} S(m) = \alpha \sum_{m=1}^{\infty} \frac{x^m}{m} = \alpha \ln\left[\frac{1}{(1-x)}\right] = \alpha \ln\left(1 + \frac{N}{\alpha}\right).$$

Thus, where the log series is obeyed, so is equation 7.1.

The number $S(m)$ of species on a small plot with m trees $\geq$10 cm dbh apiece often approximates a log series (Williams 1964). For example, the distribution of trees in hectare 7.0 of the Barro Colorado Island (BCI) Forest Dynamics Plot, with 92 species among 424 trees $\geq$10 cm dbh in 1990 approximated a log series with $\alpha = 36.17$, $x = 0.9214$ (fig. 7.1). On the other hand, the distribution of trees $\geq$10 cm dbh by species on the whole 50-hectares plot does not obey the log series: there are too few rare species. Nonetheless, in 1990 this plot contained $S = 229$ species among $N = 21{,}233$ trees $\geq$10 cm dbh. Solving $S = \alpha \ln(1 + N/\alpha)$ for α by successive approximations (Condit et al. 1998; box 7.1) yields $\alpha = 35.87$.

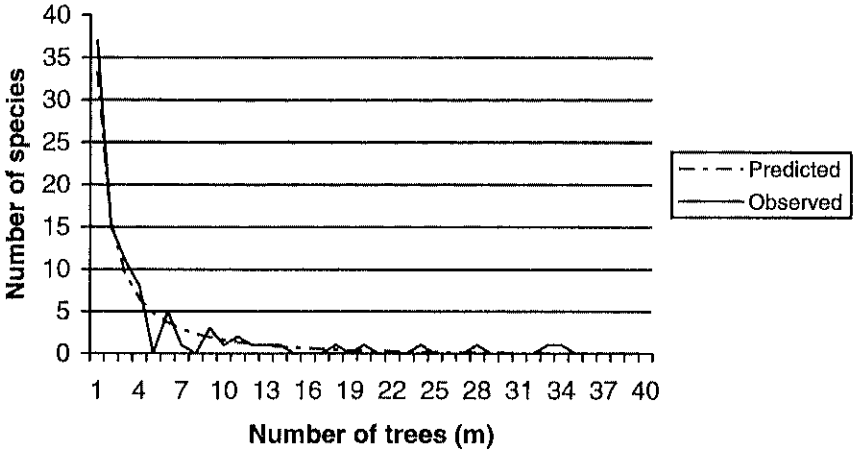

Fig. 7.1. Number of species represented on 1 ha (hectare 7.0) of the BCI Forest Dynamics Plot by m trees apiece, $S(m)$, compared with the predicted $S(m) = \alpha x^m/m$, where $\alpha = 36.17$, $x = 0.9214$.

The equation $S = \alpha \ln (1 + N/\alpha)$ does not yield a formula for α in terms of N and S. However, we may use this equation to find α by successive approximations. Let $N = 21233$, $S = 229$. Choose $\alpha_0 = 100$. Then

$$\alpha_1 = S/\ln (1 + N/\alpha_0) = 42.70; \alpha_2 = S/\ln (1 + N/\alpha_1) = 36.87$$
$$\alpha_3 = S/\ln (1 + N/\alpha_2) = 36.02; \alpha_4 = S/\ln (1 + N/\alpha_3) = 35.89$$

Because the sequence of approximations never overshoots the real value, we can check whether $\alpha > \alpha^* = 35.85$ by evaluating $S/\ln (1 + N/\alpha^*)$, which is 35.86. Thus, α has been shown to lie between 35.86 and 35.89 for $N = 21233$, $S = 229$.

Box 7.1. Finding α from N and S.

Thus the validity of equation 7.1 (as indicated by the constancy of α) transcends the validity of the log series.

In nine different Forest Dynamics Plots, S is predicted well by equation 7.1 (fig. 7.2). That is, α varies rather little with sample size (table 7.1). Fisher's α also depends relatively little on the lower diameter limit of trees sampled, as long as the sample includes over 500 trees (table 7.1). For trees over 20 cm dbh on a single hectare, Fisher's α falls below the values for larger plots or lower diameter limits. Fisher's α is much less sensitive to plot size than either the number of species S or the number S/N of species per individual on a plot (table 7.2).

For those Forest Dynamics Plots where equation 7.1 accurately describes the relation between N and S, curves for different plots should not intersect. Curves for the three most diverse plots, Lambir, Yasuní, and Pasoh, are much higher than those for other sites at all subplot sizes, while the curve for the least diverse site, Mudumalai, falls below all the others for all subplot sizes. Similarly, the curves for Barro Colorado Island, Sinharaja, and Huai Kha Khaeng do not intersect.

Equation 7.1, however, is misleading for some sites. At Mudumalai and Huai Kha Khaeng, Fisher's α increases with plot size even though, for any given plot size, it depends little on the lower diameter limit of trees sampled (table 7.1). Fisher's α is least useful at Korup and Ituri, where it increases rapidly with plot size and decreases markedly with increase in the lower diameter limit of trees sampled. Moreover, the species–individual curves for the two 10-ha mixed-forest plots and the two 10-ha monodominant forest plots at Ituri intersect the curves for Barro Colorado Island, Sinharaja, and Huai Kha Khaeng. Likewise, the Lambir curve crosses those for Pasoh and Yasuní. What causes these failures in equation 7.1?

The relationship between S and N is affected by two factors: the abundance of all the species, and the degree of spatial aggregation of individuals within each species. Species accumulation depends on abundances as follows. If all species are equally abundant, sampling is extremely efficient, and small samples will have many of the species present. In contrast, consider the extreme where one

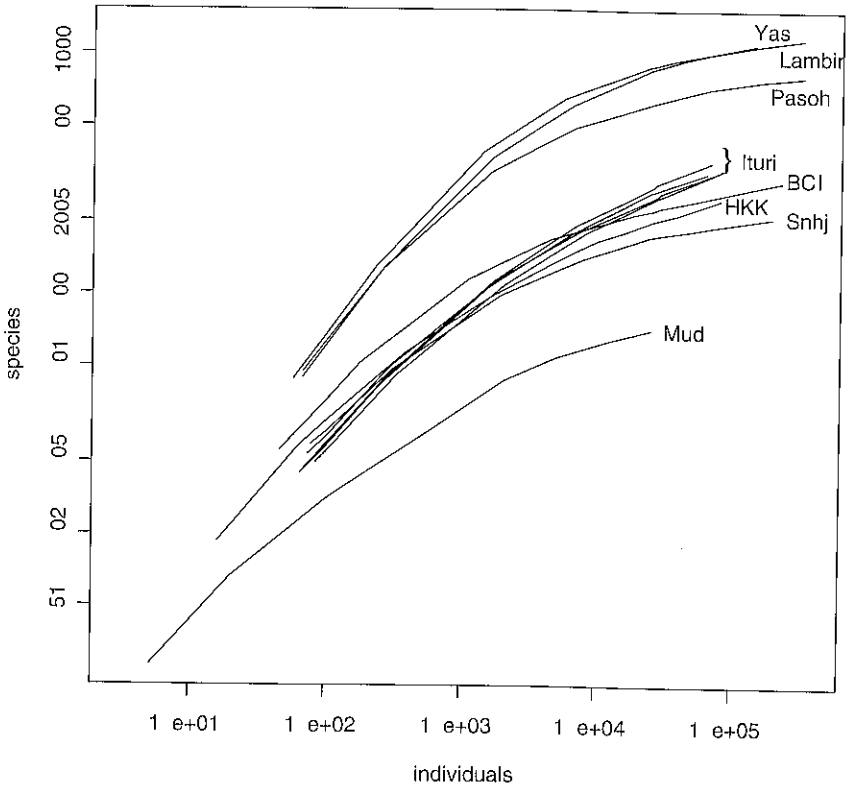

Fig. 7.2. Species accumulation curves at eight different sites, including four different plots at Ituri in Africa. The curves were calculated as described in Condit et al. (1996), using square quadrats of 10, 20, 50, 100, 200, 250, and 500 m on a side (the last two could not be done in the Ituri plots, though, which are 200 × 500 m rectangles). The rightmost point in all lines represents the entire plot, whether square or rectangle. For BCI, the 1995 census was used; for all other plots, the initial census was used.

species is extremely abundant and all others are rare. Sampling is then extremely inefficient—small samples have few species, and the rare species appear slowly. This contrast suggests a simple way to assess the form of the species accumulation curve: calculate the ratio of the number of species found in a small sample to the number found in a large sample. With an even abundance distribution, this ratio will be a relatively high number; but with very uneven abundances, it will be much lower.

We will use this efficiency ratio below to characterize the form of the species accumulation curve at all plots and then to judge which factors are responsible for causing the accumulation curves in figure 7.2 to deviate from the prediction of

Table 7.1. Different Diameter Thresholds on Different-Sized Subplots of CTFS Forest Dynamics Plots

	1 ha			6.25 Ha			25 Ha		
Plot	*N*	*S*	α	*N*	*S*	α	*N*	*S*	α
Sinharaja									
Trees ≥1 cm	8,214	141	24.5	51,337	186	24.3	205,373	205	22.5
≥5 cm	1,427	94	22.7	8,918	151	25.8	35,681	187	25.9
≥10 cm	677	69	19.5	4,234	126	24.3	16,937	167	25.7
≥20 cm	284	48	16.7	1,774	97	22.0	7096	138	24.3
	N	*S*	α	*N*	*S*	α	*N*	*S*	α
Yasuní									
Trees ≥1 cm	6,094	655	187	38,089	950	177	152,360	1,104	161
≥5 cm	1,611	413	181	10,071	759	190	40,284	954	175
≥10 cm	702	251	142	4,387	579	179	17,546	820	178
≥20 cm	219	115	101	1,369	347	150	5,476	590	168
	N	*S*	α	*N*	*S*	α	*N*	*S*	α
Lambir									
Trees ≥1 cm	6,907	618	165	43,170	955	173	172,679	1,120	160
≥5 cm	1,471	387	174	9,196	759	197	36,782	985	186
≥10 cm	637	247	154	3,979	591	194	15,916	851	193
≥20 cm	234	120	109	1,462	359	157	5,848	620	179
	N	*S*	α	*N*	*S*	α	*N*	*S*	α
Pasoh									
Trees ≥1 cm	6,707	495	124	41,918	681	116	167,673	781	106
≥5 cm	1,375	327	136	8,595	556	133	34,380	694	123
≥10 cm	531	206	125	3,319	440	136	13,276	604	130
≥20 cm	169	92	86	1057	260	110	4,229	439	123
	N	*S*	α	*N*	*S*	α	*N*	*S*	α
BCI									
Trees ≥1 cm	4,581	169	34.6	28,631	230	34.2	114,524	275	33.8
≥5 cm	1,024	128	39.0	6,401	199	39.0	25,603	242	36.9
≥10 cm	429	91	35.6	2,682	162	37.9	10,728	206	36.1
≥20 cm	156	53	28.5	978	114	33.4	3911	162	34.1
	N	*S*	α	*N*	*S*	α	*N*	*S*	α
HKK									
Trees ≥1 cm	1,450	96	23.3	9,064	166	28.9	36,255	218	30.8
≥5 cm	738	81	23.2	4,610	150	29.8	18,441	202	31.7
≥10 cm	438	65	21.3	2,734	130	28.5	10,938	185	31.5
≥20 cm	171	44	19.7	1,070	99	26.5	4,281	150	30.3
	N	*S*	α	*N*	*S*	α	*N*	*S*	α
Mudumalai									
Trees ≥1 cm	353	23.9	5.9	2,204	46.8	8.4	8,815	63	9.2
≥5 cm	315	22.9	5.9	1,970	44.9	8.2	7,882	60	8.9
≥10 cm	281	21.4	5.5	1,756	43.1	8.0	7,024	58	8.7
≥20 cm	180	18.0	5.1	1,123	37.1	7.4	4,494	53	8.5
	N	*S*	α	*N*	*S*	α	*N*	*S*	α
Korup									
Trees ≥1 cm	6,581	236	48.0	41,128	353	53.0	164,513	441	55.1
≥5 cm	1,319	134	37.6	8,243	241	46.5	32,970	332	51.3
≥10 cm	492	87	30.8	3,074	181	42.1	12,296	261	46.7
≥20 cm	192	54	25.3	1199	126	35.6	4796	200	42.1

(Continued)

Table 7.1. (Continued)

Plot	1 ha			6.25 Ha			25 Ha		
	N	S	α	N^*	S^*	α^*	N^{**}	S^{**}	α^{**}
Ituri (Monodominant Forest)									
Trees ≥1 cm	6,843	159	29.2	26,943	218	32.4	68,431	272	36.0
≥5 cm	940	90	24.8	3,676	145	30.1	9,403	208	37.6
≥10 cm	358	53	17.7	1,382	91	22.1	3,576	159	34.0
≥20 cm	151	22	7.9	605	50	13.5	1,511	100	24.0
	N	S	α	N^*	S^*	α^*	N^{**}	S^{**}	α^{**}
Ituri (Mixed Forest)									
Trees ≥1 cm	8,112	149	26.0	33,275	214	30.6	81,115	252	32.2
≥5 cm	1,301	94	23.2	5,289	154	29.8	13,010	194	32.3
≥10 cm	438	64	20.7	1,751	114	27.2	4,381	151	30.2
≥20 cm	127	36	17.3	508	79	26.1	1,272	115	30.6

Note: Average number of trees N, Number of Species S, and Fisher's α above.

*Subplots are 4.0 ha (200 × 200 m) and are averaged across both 10-ha Ituri Forest Dynamics Plot in each forest type.
**Subplots are 10.0 ha (200 × 500 m) and the average of both 10-ha Ituri Forest Dynamics Plot in each forest type.

equation 7.1 (which we refer to as the neutral prediction; see below). Specifically, we define the efficiency ratio as

$$R = \frac{S_{100}}{S_{25000}} \tag{7.2}$$

where S_{100} is the number of species found in a square quadrat with 100 individuals, and S_{25000} is the number found in a square quadrat with 25,000 individuals. The number 25,000 was chosen because the Mudumalai plot has just more than 25,000 individuals—it is the largest sample available in all plots; 100 was chosen arbitrarily to represent a small sample. Efficiency ratios were quite low (<10%) in all four Ituri plots and higher at BCI (16%; see table 7.3).

The second factor affecting the accumulation curve is spatial aggregation. If all species are uniformly spaced across a plot, then sampling is most efficient. Small samples will include many of the species, and the efficiency ratio will be high. But if species are highly aggregated, sampling is least efficient. In an extreme case—for example, where species occur in clumps that do not overlap—a sample smaller than the clump size would seldom have more than three species.

There are two different mechanisms that can cause aggregation: dispersal limitation and habitat preference (Condit et al. 2000). Both have a similar effect on the species accumulation curve, although habitat preference should have a more pronounced impact because it can lead to less intermingling of species distributions. In the current analysis, though, we cannot distinguish between the two mechanisms, so we only consider the importance of aggregated distributions in general.

Table 7.2. Number N of Trees ≥10 cm dbh, Number S of Species among Them, and Fisher's α in the Average 500 × 500 m Subplot, or the Whole Plot if Smaller, and the Average 100 × 100 m Subplot at Each Forest Dynamics Plot

	N	S	S/N	N	S	S/N
	500 × 500 m			100 × 100 m		
Lambir, Sarawak[†]	15,916	851	0.053	637	247	0.388
Pasoh, Malay Peninsula	13,276	604	0.046	531	206	0.390
HKK, Thailand	10,938	185	0.017	438	65	0.148
Mudumalai, South India	7,024	58	0.008	281	21	0.075
Sinharaja, Sri Lanka	16,937	167	0.010	677	69	0.102
Korup, Cameroon	12,296	261	0.021	492	87	0.177
Yasuní, Ecuador	17,546	820	0.047	702	251	0.358
La Planada, Colombia	14,650	179	0.012	586	88	0.150
Barro Colorado, Panama	10,728	206	0.019	429	91	0.212
	500 × 320 m			100 × 100 m		
Luquillo, Puerto Rico	13,988	86	0.006	876	42	0.048
	500 × 200 m			100 × 100 m		
Ituri (Mixed Forest), D.R. Congo	4,381	151	0.034	438	64	0.146

[†]The Lambir tree counts include only identified trees.

How can we separate the impact of the abundance distribution and spatial aggregation on the species accumulation curve? First, we use Hubbell's theory to predict a species–individual curve, which is very nearly equation 7.1 (see above). For each plot, the neutral species accumulation curve was calculated from equation 7.1, after finding α for the full plot (table 7.3), following the method given in Condit et al. (1998). Then the expected efficiency ratio (eq. 7.2) under the neutral model can be calculated with the use of equation 7.1, plugging in $N = 100$ and then $N = 25{,}000$ (actually, $N = 101$ and 25,344 at BCI, and likewise for the other plots; see table 7.3 notes).

The expected efficiency ratios under the neutral model vary with total species richness. In the three very diverse plots (Lambir, Pasoh, Yasuní), $R < 0.12$; it is about 0.2 in the middiversity plots; and >0.3 at Mudumalai (table 7.3, fig. 7.3). Thus, the efficiency of sampling species varies with species diversity even under the null model. Species are encountered more efficiently in small samples when diversity is low. This is an intuitive result, since species will be more abundant in a less diverse forest, assuming that abundance distributions have the shape that the neutral model predicts.

In all forests, observed species accumulation curves are less efficient—that is, the efficiency ratio is lower—than expected under the neutral model (fig. 7.3). For example, the efficiency ratio of the species accumulation curve at Yasuní would be 9.5% if a forest of the same species richness obeyed the predictions of the null model. The observed ratio is 7.4%. Is this because the abundance distribution differs from the prediction of the null theory, or because species are aggregated

Table 7.3. Number of Species in Square Plots Holding 100 Individuals and 25,000 Individuals in 11 Different Forest Dynamics Plots

	$N = 100$ Individuals			$N = 25{,}000$ Individuals			α	Top 3	Efficiency Ratio		
	Dimen.	Species	Individ.	Dimen.	Species	Individ.	Full Plot	Species	Neutral	Abund.	Observ.
BCI	14.8	35.4	100.7	233.6	224.9	25,343.5	33.9	0.332	0.209	0.179	0.158
Yasuní	13.1	67.2	100.7	207.3	903.5	25,733.3	162.4	0.070	0.095	0.085	0.074
Ituri-Mixed Forest 1	11.5	25.2	100.6	181.1	257.0	26,449.0	43.4	0.540	0.190	0.121	0.098
Ituri-Mixed Forest 2	10.8	21.9	100.0	170.5	253.5	26,975.0	43.7	0.633	0.188	0.104	0.086
Ituri-Mono Forest 1	11.9	23.5	99.9	187.7	280.5	25,203.0	49.0	0.608	0.179	0.097	0.084
Ituri-Mono Forest 2	12.3	22.9	99.2	194.8	268.5	24,765.5	44.3	0.580	0.185	0.102	0.085
HKK	25.0	29.9	101.2	395.8	203.5	25,728.0	31.7	0.258	0.213	0.188	0.147
Lambir	12.2	60.8	100.2	193.1	867.2	24,331.6	152.6	0.070	0.099	0.081	0.070
Mudumalai	44.5	13.9	100.5	1000×500	71.0	25,250.0	8.9	0.465	0.312	0.227	0.195
Pasoh	12.2	62.9	100.5	193.1	631.8	25,816.3	100.3	0.074	0.125	0.100	0.100
Sinharaja	11.3	26.7	101.2	178.6	172.8	23,952.8	23.2	0.269	0.240	0.239	0.154

Notes: We found the observed number of species by choosing quadrat dimensions that would include just 100 or just 25,000 trees. At BCI, for example, quadrats of 233.6×233.6 m have close to 25,000 individuals. These dimensions were found as the square area that would include 25000 individuals given the density of trees in all 50 ha. The actual number of individuals in the four nonoverlapping quadrats of 233.6×233.6 m that can be placed adjacent to one another within the plot, starting in the southwest corner, turned out to average 25,343.5, slightly more than 25,000 because the four quadrats do not encompass the entire plot. It was not necessary to be more precise than this, and in estimates of the expected efficiency ratio (see above) at BCI, $N = 25.344$ was always used instead of $N = 25{,}000$. These are given for each plot. Fisher's α is given for each plot, and the fraction of trees belonging to the three most abundant species. The final three columns give the efficiency ratio from the species individual curve—species in 100 individuals divided by species in 25,000 individuals. First is the efficiency ratio under the neutral assumption, then the ratio of species among 100 trees to species among 25,000 trees, sampled at random from the whole plot, and finally the observed ratio. Plots are listed geographically, first the two in the New World, then four plots in Africa, and finally five in Asia. The four African plots are all at a single location in the Ituri forest.

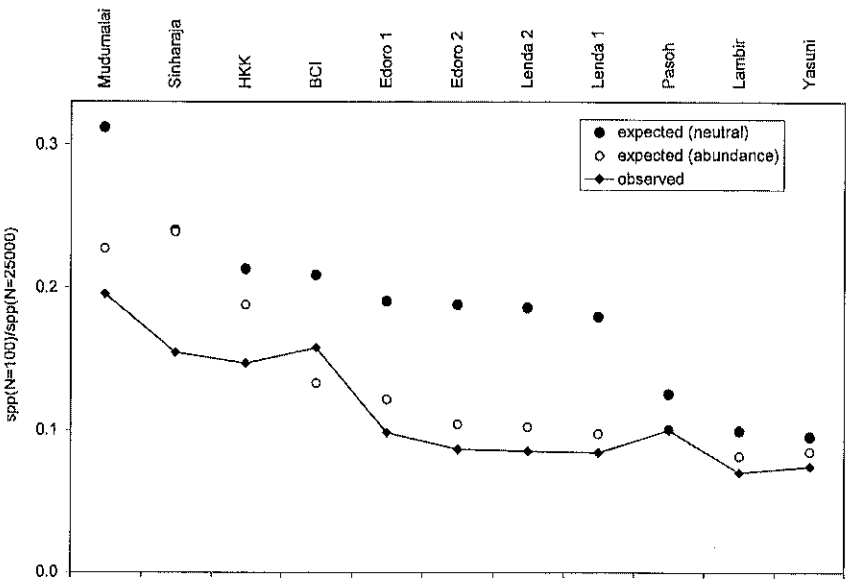

Fig. 7.3. The efficiency ratio of the species–individual curve, observed and predicted from two sets of assumptions. The first prediction is from the neutral theory and is thus based on equation 7.1. The second prediction is from the abundance distribution, following equation 7.3.

spatially? One more calculation allows us to answer this question. The impact of aggregation can be separated from the impact of the abundance distribution by calculating the species–individual curve using random subsets of individuals drawn from the observed species' abundances. This removes any impact of spatial arrangements, and it can be done analytically using the derivation presented in Hurlbert (1971),

$$S_n = S - \sum_{i=1}^{S} \prod_{j=0}^{n-1} \left(\frac{N - a_i - j}{N - j} \right), \tag{7.3}$$

where S_n is the number of species in n individuals, S is the total species in the full sample of N individuals, and a_i is the abundance of the ith species. Equation 7.3 was used to calculate S_{100} and S_{25000} in all plots. (Again, the exact numbers differed slightly from 100 and 25000 and are given in table 7.3).

Figure 7.3 gives the observed efficiency ratios for all plots, as well as the expected values under the neutral theory (eq. 7.1, and as calculated from the observed distribution of abundances for the whole plot using the rarefaction equation 7.3). The impact of abundance can be gleaned from figure 7.3 by comparing the neutral prediction (black circle) with the prediction from the observed abundance

distribution (open circle). In most plots, the abundance distribution causes the greatest deviation from neutral, with the largest impact at the four plots in Ituri (Edoro 1 and 2 and Lenda 1 and 2), at Barro Colorado, and at Mudumalai. Table 7.3 shows that these plots also have the most dominated abundance distributions, with a few species occupying a high percentage of the forest (and thus deviating most from the abundance distribution predicted by the null model). At a few sites, the abundance distributions must be close to the prediction of the neutral model, especially at Sinharaja, where changing the abundance distribution had no effect on the efficiency ratio (fig. 7.3).

The effect of species aggregation was generally less important than that of the abundance distribution (fig. 7.3). At Pasoh, aggregation had no impact on the efficiency ratio, and indeed, this forest had a very low measure of species aggregation relative to the other plots. In contrast, at Sinharaja, Huai Kha Khaeng, and Lambir, aggregation had a greater impact than the abundance distribution in determining the efficiency ratio, and sure enough, these three forests had the highest indices of aggregation (Condit et al. 2000).

In summary, Fisher's α would be a perfect diversity index if the species accumulation curve were predicted by equation 7.1; then α would be independent of sample size and could be used to extrapolate species richness to large areas. The deviation between this prediction and the observed accumulation curve is indicated by the efficiency ratio in figure 7.3. The deviation is fairly small for BCI, Pasoh, and Yasuní, but substantial at other sites. In most forests, the failure of α to predict species accumulation can be attributed mostly to the abundance distribution, which deviates from the prediction of the neutral model in being more uneven (more very abundant species and more very rare species). Species aggregation, including dispersal clumps or habitat preferences, produces further deviations from expected, although with a smaller impact than the abundance distribution in most forests.

References

Condit, R., P. S. Ashton, P. Baker, S. Bunyavejchewin, S. Gunatilleke, N. Gunatilleke, S. P. Hubbell, R. B. Foster, L. Hua Seng, A. Itoh, J. V. LaFrankie, E. Losos, N. Manokaran, R. Sukumar, and T. Yamakura. 2000. Spatial patterns in the distribution of tropical tree species. *Science* 288:1414–18.

Condit, R., R. B. Foster, S. P. Hubbell, R. Sukumar, E. G. Leigh, N. Manokaran, and S. Loo de Lao. 1998. Assessing forest diversity on small plots: Calibration using species–individual curves from 50 ha plots. Pages 247–68 in F. Dallmeier and J. A. Comiskey, editors. *Forest Biodiversity Research, Monitoring, and Modeling*. Man and the Biosphere Series. Parthenon Publishing, Pearl River, NY.

Condit, R., S. P. Hubbell, J. V. LaFrankie, R. Sukumar, N. Manokaran, R. B. Foster, and P. S. Ashton. 1996. Species–area and species–individual relationships for tropical trees: A comparison of three 50 ha plots. *Journal of Ecology* 84:549–62.

Fisher, R. A., A. S. Corbet, and C. B. Williams. 1943. The relation between the number of species and the number of individuals in a random sample of an animal population. *Journal of Animal Ecology* 12:42–58.

Hubbell, S. P. 1997. A unified theory of biogeography and relative species abundance and its application to tropical rain forests and coral reefs. *Coral Reefs* 16(Suppl.):S9–S21.

———. 2001. *The Unified Neutral Theory of Biodiversity and Biogeography.* Princeton University Press, Princeton, NJ.

Hurlbert, S. H. 1971. The nonconcept of species diversity: A critique and alternative parameters. *Ecology* 52:577–86.

Rosenzweig, M. L. 1995. *Species Diversity in Space and Time.* Cambridge University Press, New York.

Watterson, G. A. 1974. Models for the logarithmic species abundance distribution. *Theoretical Population Biology* 6:217–50.

Williams, C. B. 1964. *Patterns in the in the Balance of Nature.* Academic Press, London.

Condit, R., S. P. Hubbell, J. V. LaFrankie, R. Sukumar, N. Manokaran, R. B. Foster, and P. S. Ashton. 1996. Species–area and species–individual relationships for tropical trees: A comparison of three 50 ha plots. *Journal of Ecology* 84:549–62.

Fisher, R. A., A. S. Corbet, and C. B. Williams. 1943. The relation between the number of species and the number of individuals in a random sample of an animal population. *Journal of Animal Ecology* 12:42–58.

Hubbell, S. P. 1997. A unified theory of biogeography and relative species abundance and its application to tropical rain forests and coral reefs. *Coral Reefs* 16(Suppl.):S9–S21.

———. 2001. *The Unified Neutral Theory of Biodiversity and Biogeography.* Princeton University Press, Princeton, NJ.

Hurlbert, S. H. 1971. The nonconcept of species diversity: A critique and alternative parameters. *Ecology* 52:577–86.

Rosenzweig, M. L. 1995. *Species Diversity in Space and Time.* Cambridge University Press, New York.

Watterson, G. A. 1974. Models for the logarithmic species abundance distribution. *Theoretical Population Biology* 6:217–50.

Williams, C. B. 1964. *Patterns in the in the Balance of Nature.* Academic Press, London.